

Bronze Age Northern Eurasian Genetics in the Context of Development of Metallurgy and Siberian Ancestry

Ainash Childebayeva^{1,2*}, Fabian Fricke³, Adam Benjamin Rohrlach^{1,4}, Lei Huang¹, Stephan Schiffels¹, Outi Vesakoski⁵, Lena Semerau¹, Franziska Aron⁶, Vyacheslav Moiseyev⁷, Valery Khartanovich⁷, Igor Kovtun⁸, Johannes Krause¹, Sergey Kuzminykh⁹, Wolfgang Haak^{1*}

¹*Department of Archaeogenetics, Max Planck Institute for Evolutionary Anthropology, D-04103 Leipzig, Germany*

²*Department of Anthropology, University of Kansas, Lawrence, KS 66044, USA*

³*German Archaeological Institute, Eurasia Department, Berlin 14195, Germany*

⁴*School of Computer and Mathematical Sciences, University of Adelaide, Adelaide SA 5005, Australia*

⁵*Department of Finnish and Finno-Ugric Languages, University of Turku, Turku 20014, Finland*

⁶*Department of Archaeogenetics, Max Planck Institute for the Science of Human History, Jena 07745, Germany*

⁷*Peter the Great Museum of Anthropology and Ethnography (Kunstkamera), Russian Academy of Sciences, University Embankment, 3, Saint Petersburg 199034, Russia*

⁸*T.F. Gorbachev Kuzbass State Technical University, Department of History, Philosophy and Social Sciences, Kemerovo 650000, Russia*

⁹*Russian Academy of Sciences, Institute of Archaeology, Laboratory of Natural Scientific Methods, Moscow 117292, Russia*

* Corresponding authors:

Ainash Childebayeva (ainash_childebayeva@eva.mpg.de), Wolfgang Haak (wolfgang_haak@eva.mpg.de)

Author Contributions:

Conceptualization: WH, AC

Methodology: LS, FA

Investigation: AC, WH, FF, ABR, LH

Visualization: AC, WH, FF

Supervision: WH, JK, SS

Resources: FF, VM, VK, IK, SK

Writing—original draft: AC, WH

Writing—review & editing: WH, AC, ABR, FF, LH, SK, OV

Competing Interest Statement: We do not have any competing interests

36 **Classification:** Social sciences, Anthropology, Population Genetics.

37 **Keywords:** ancient DNA, Bronze Age Eurasia, Siberian Ancestry, population genetics.

38

39 **This PDF file includes:**

40 Main Text

41 Figures 1 to 6

42 Tables 1

43

44 **Abstract**

45

46 The Eurasian Bronze Age (BA) has been described as a period of substantial human
47 migrations, the emergence of pastoralism, horse domestication, and development of
48 metallurgy. This study focuses on individuals associated with BA metallurgical production,
49 specifically the Seima-Turbino (ST) phenomenon (~2,200-1,900 BCE) associated with
50 elaborate metal objects found across Northern Eurasia. The genetic profiles of nine ST-
51 associated individuals vary widely ranging between ancestries maximized in individuals from
52 the Eastern Siberian Late Neolithic/BA, and those of the Western Steppe Middle Late BA. The
53 genetic heterogeneity observed is consistent with the current understanding of the ST
54 metallurgical network as a transcultural phenomenon. The new data also shed light on the
55 temporal and spatial range of an ancient Siberian genetic ancestry component, which is shared
56 across many Uralic-speaking populations, and which we explore further via demographic
57 modeling using additional genome-wide (2 individuals) and whole genome data (5 individuals,
58 including a ~30x genome) from northwestern Russia.

59

60 **Introduction**

61

62 Bronze Age Eurasia (~3000-1000 BCE) is characterized by the development of metallurgy,
63 one of the most important cultural innovations in human history. The Early Bronze Age in
64 Eurasia (~3000 BCE) is associated with the emergence of the Circumpontic Metallurgical
65 Province, and eastward expansion of metallurgical production and exchange across the
66 Eurasian steppe¹⁻³. In the Late Bronze Age (~2200–1000 BCE), a westward movement of
67 materials was also detected, specifically in connection with the so-called Seima-Turbino
68 (henceforth ST) phenomenon^{1,2} as seen by the presence of specific metal artifacts throughout
69 the forest and forest-steppe regions of Northern Eurasia⁴.

70

71 The ST is represented by several sites throughout Eurasia dating to ~2,200-1,900 BCE and
72 constitutes a “metallurgical network” represented by many shared traits, such as the use of tin-
73 copper, comparable artifact types, and shared metallurgical technologies that may have
74 involved a movement of craft workers and/or groups^{4,5}. The ST has been described as a
75 “transcultural” phenomenon, i.e., a network of metallurgical production with shared traits on
76 top of the underlying basis of consistent pottery types in the different areas associated with
77 various archaeological cultures throughout northern Eurasia.

78

79 The name Seima-Turbino derives from the two eponymous burial grounds Seima and Turbino
80 excavated in the beginning of the 20th century CE⁴. The ST phenomenon combines elements
81 of several cultures and does not represent a single culture in itself, especially since there are
82 no distinct settlements or pottery styles associated with it. Instead, certain metal objects, which
83 were found throughout Eurasia, from China and Central Asia in the East to Finland and
84 Moldova in the West, spanning across approximately three million square kilometers,
85 represent key ST-associated criteria (see Supplementary Note 1, Figure 1, and Supplementary
86 Figure 1). In the entire spatial distribution of the ST, there is a certain degree of regional
87 variation (see Supplementary Note 1). Briefly, the artifacts in the east contain higher amounts
88 of tin (Sn) (Supplementary Figures 2 and 3) and more casting molds have been identified in
89 the east compared to the west of the Urals, although a greater number and variation of ST
90 objects have been found west of the Urals (Figure 1c). The metallic inventory of ST-complexes
91 can be divided into two major groups: (1) objects that can be attributed to Eurasian
92 archaeological cultures, such as Alakul, Abashevo, Sintashta, Petrovka and Srubnaya; (2)
93 objects that are only known from ST-sites (socket axes, lamellar dagger blades, fully hilted
94 daggers and knives and the so-called forked lanceheads) (Figure 1c). Singular finds of objects
95 and weaponry of the ST type have been reported from contexts otherwise attributed to Bronze
96 Age Glazkovo, Okunevo, Elunino, Odino, Krotovo, Koptyaki, Sintashta, Petrovka, Abashevo,
97 Srubnaya (Pokrovka), and Post-Fatyanovo cultures^{4,6}. However, these finds are rare and most
98 ST materials are found at ST-associated sites.

99
100 The people buried with ST-objects have been described as metallurgists who developed
101 elaborate and distinct bronze objects, and possibly used river systems for transportation⁴.
102 Even though the horse plays a central role in the ST iconography, it remains unclear whether
103 people associated with the phenomenon were using horses for riding, traction or transport. It
104 has been hypothesized that the number of people associated with the ST phenomenon was
105 small, since there are very few sites with human remains linked to the phenomenon, and ST
106 metal artifacts are comparably few but geographically widespread. ST burials are very distinct
107 from those of the other North Eurasian cultures: individuals were buried mostly without pottery
108 and not in kurgans, both inhumations and cremations were common, and the grave goods
109 included bronze, stone, and bone weaponry, as well as bone armor. In cases where pottery is
110 present at ST-sites, it can be attributed to other local cultures, for example Koptyaki at the site
111 Shaitanskoe Ozero II⁷. The early history of the ST phenomenon is not well understood,
112 however, based on the presence of tin and copper in metal alloys of ST objects, the Altai and
113 Tian-Shan mountains have been proposed^{4,8}.

114

115 Here, we present ancient human DNA data from a well-known, ST-associated site Rostovka
116 (ROT), which is one of the very few ST sites with preserved human remains. The majority of
117 the graves found at Rostovka contain bronze ST objects, bronze weapons and tools, casting
118 molds, jewelry, bone knife handles, and armor plates⁹. In fact, the majority of Rostovka burials
119 contain weapons, found in 60% of the female and 80% of the male burials¹⁰. The radiocarbon
120 dates for Rostovka, excluding extreme values, range between ca. 2200-2000 cal. BCE^{3,9,11}.
121 This chronological horizon is simultaneous with the Okunevo culture, while its lower bound
122 overlaps with the early Abashevo and Sintashta cultures, among others (Fig. 1b).

123

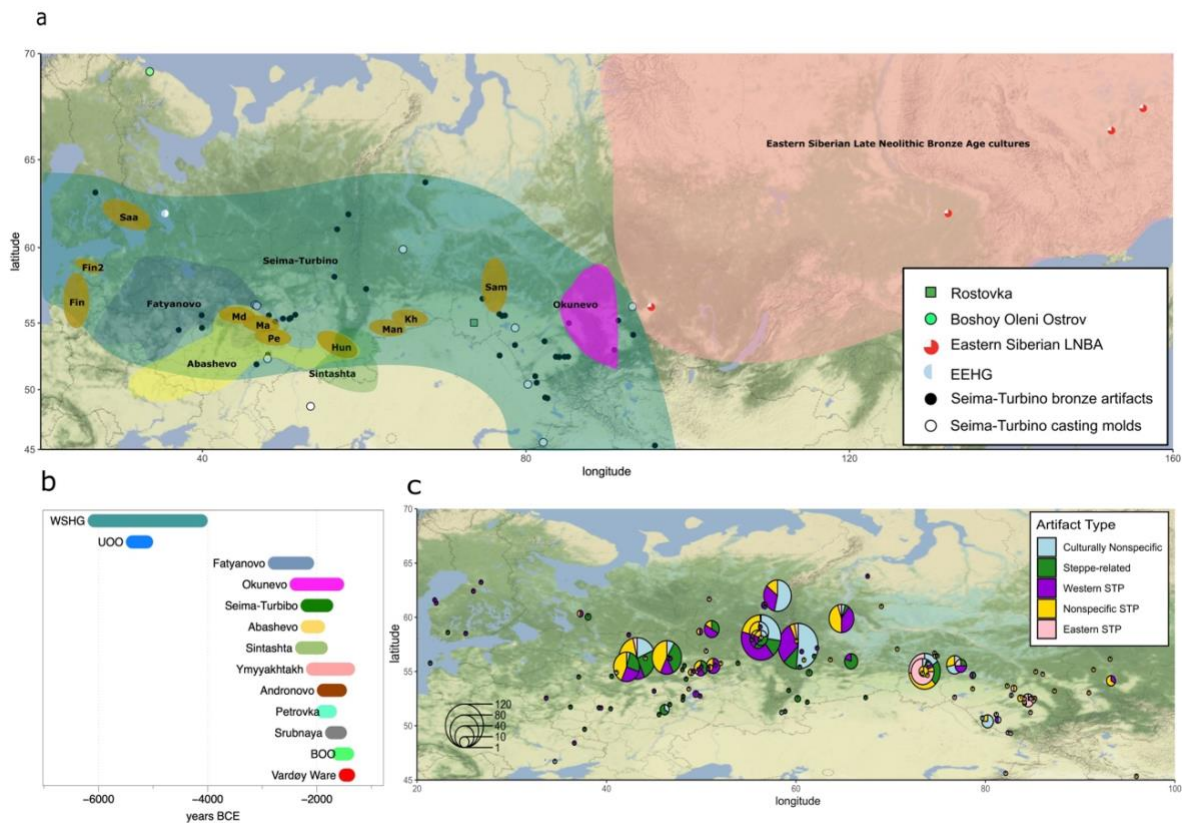
124 An identifying component in the genetic landscape of Northern Eurasia is a shared Siberian
125 ancestry component, which is present in the genetic profiles of Finnish, Estonian, Saami-
126 speaking, and indigenous Siberian populations today¹². A previous ancient DNA study focusing
127 on the Eastern Baltic found a genetic contribution from Siberia in the Iron Age but not in the
128 Bronze Age, which was linked to the time of the arrival of Uralic languages to the region¹³.
129 Moreover, the Y-haplogroup N1a1a1a1a (previously known as N3a), primarily found in
130 present-day northern Eurasian and Uralic speaking groups, first appears in Europe in Early
131 Metal Age individuals from the Bolshoy Oleni Ostrov site (BOO)¹⁴, in northwestern Russia,
132 together with evidence of high levels of genome-wide Siberian ancestry¹⁵.

133

134 We present new genome-wide data from two additional BOO individuals and shotgun data for
135 five published individuals (including one high coverage genome of ~31x). Direct or indirect
136 contacts between BOO and southern and western Scandinavia have been proposed based on
137 genetic data and the archaeological record¹⁴⁻¹⁶, but BOO has not been associated with any
138 known early Metal Age cultures.

139

140 Here, we report the results of joint population genetic analyses of both sites in comparison with
141 published ancient data from chronologically, geographically, and archaeologically relevant
142 cultures of the forest-tundra (taiga and tundra) and forest-steppe zones of Eurasia. We also
143 investigate the demographic history of Northern Eurasia, especially in context of the Siberian
144 genetic component. Together, we aim to provide an updated view on the genetic history and
145 connections of populations of the forest-steppe and western Siberia, with an emphasis on the
146 ST phenomenon in the context of metallurgical production.



147

148 **Figure 1.** (a) Geographic map with ROT and BOO indicated, also showing hypothetical origin
 149 locations for ancestral stages of Uralic subfamilies (Saa=Saami, Fin/Fin2=Finnic, Man=Mansi,
 150 Kh=Khanty, Sam=Samoyedic, Hun=Hungarian, Md=Mordvin, Ma=Mari, Pe=Permic), and a
 151 distribution of contemporaneous archaeological cultures (adapted from Grünthal et al. 2022),
 152 (b) Chronology of Seima-Turbino (ST is including ROT) and BOO individuals together with
 153 relevant Bronze Age groups of Northern Eurasia. The timeline is based on a combination of
 154 absolute (^{14}C) and relative dates, (c) Cultural/regional attribution of the metallic inventory of
 155 the sites of the ST phenomenon. Pie charts indicate the breakdown of artifacts at specific sites
 156 by cultural/regional attribution.

157

158

159
160

Table 1. General overview of the ROT and BOO individuals included in the study.

Sample	Gen. sex	1240k SNPs	Shotgun coverage	Y hg	Y hg terminal SNP	MT hg	Date
ROT002	YV	311,602	-	N1a1a1a1a	L392	C2a1	1028-1700 calBC ($\pm 2\sigma$)*
ROT003	XY	40,320	-	R1a1a1	M417	R1a1a	ca. 4150-3800 BP, stratigraphic context
ROT004	YV	104,706	-	C1b	M246	H1	2202-1082 calBC ($\pm 2\sigma$)*
ROT006	XY	33,591	-	R1b1a1a	M73	A10	ca. 4150-3800 BP, stratigraphic context
ROT011	YV	44,705	-	C2a	L1272	C1	2051-1174 calBC ($\pm 2\sigma$)*
ROT013	XX	25,543	-	-	-	R1b1	ca. 4150-3800 BP, stratigraphic context
ROT015	YV	116,504	-	C2a1a1	F0002	C1a	2122-1010 calBC ($\pm 2\sigma$)*
ROT016	XY	257,502	-	R1a1a1b	Z645	U5a1+@1619 2	2137-1919 calBC ($\pm 2\sigma$)* ca. 4150-3800 BP
BOO001	XX	-	2.4x	-	-	U4a1***	-
BOO004	XY	-	31.8x	N1a1a1a1a	L392	C4b***	1735-1538 calBC ($\pm 2\sigma$)
BOO006	XX	-	2.6x	-	-	D4e4***	-
BOO008	YV	606,672	-	-	-	Z1a1a	-
BOO009	XX	814,966	-	-	-	U5a2	925-830 calBC ($\pm 1\sigma$)** from charcoal

161 *from ⁹

162 **from ¹⁶

163 ***from ¹⁵

164 Gen. sex=genetic sex, 1240k SNPs = SNP coverage on the 1240k array, Y hg = Y
165 chromosome haplogroup, MT hg = mtDNA haplogroup.

166

167 Results

168

169 In this study, we report genome-wide SNP data for nine individuals from the ST site Rostovka,
170 as well as additional new data for two BOO individuals (plus shotgun genome data for five
171 already published individuals) (Fig. 1a). We performed 1240k SNP^{17,18} and mitochondrial
172 genome captures on the nine individuals from ROT, and the two new BOO individuals, as well
173 as Y-chromosomal capture¹⁹ on just the males. Lastly, we generated shotgun sequence data
174 for five published BOO individuals, including one 31.8x covered individual (Fig. 1a, Table 1,
175 Supplementary Table 1). Of the newly analyzed individuals, eight ROT individuals were
176 genetically male and one was female, while both new BOO individuals were female (Table 1).
177 Biological relatedness analysis of the newly reported individuals was performed using READ²⁰
178 and IcMLkin²¹. Based on these analyses, we identified a pair of second-degree relatives
179 (ROT011 and ROT015), both of whom are males carrying the Y-haplogroup C2a, and could
180 either represent a grandson/grandparent, a nephew/uncle pair or paternal half-siblings,
181 consistent with overlapping radiocarbon dates for both individuals (Table 1). A second-degree
182 related pair was also found among the BOO individuals (BOO004-BOO005).

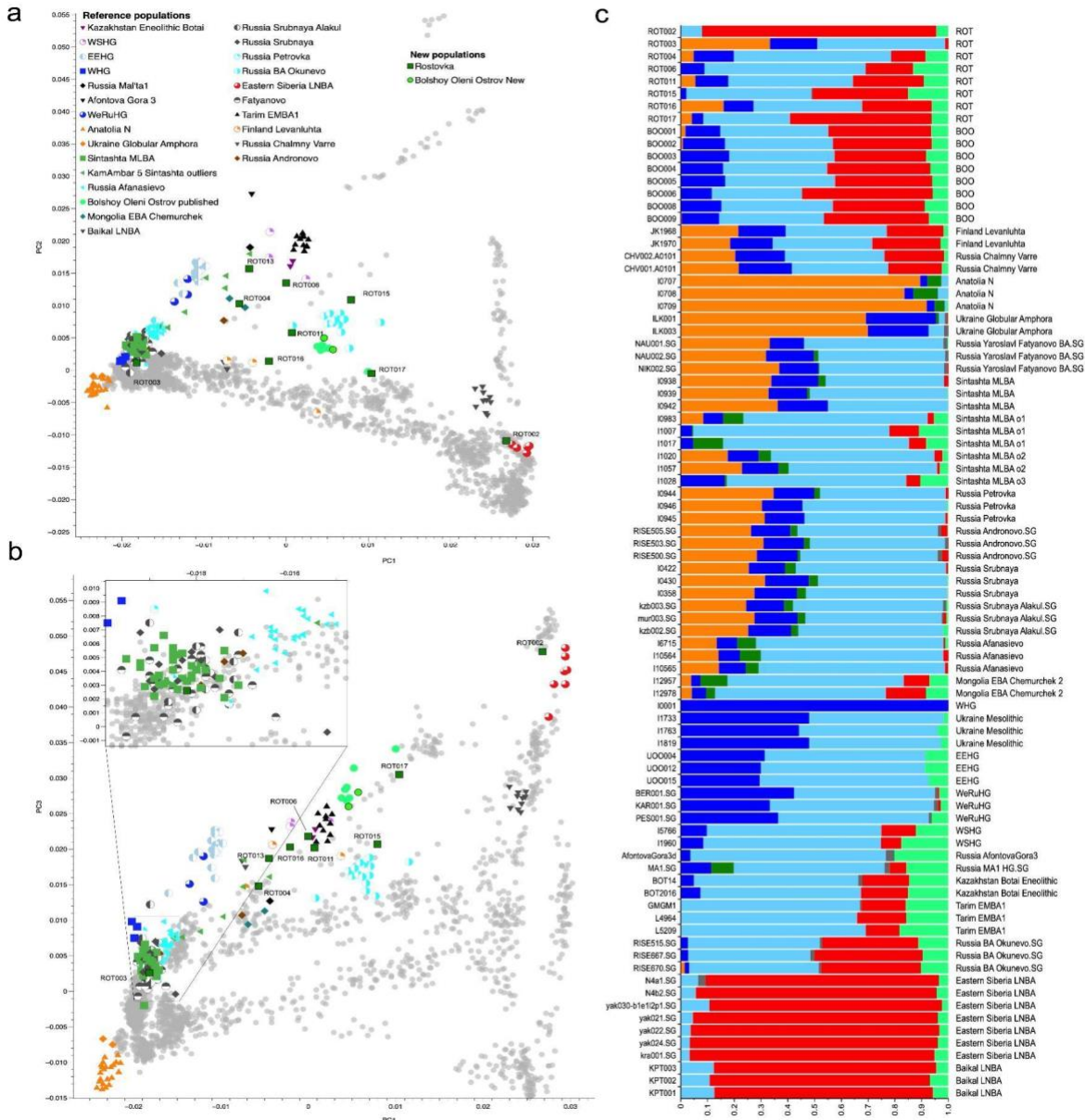
183 We also generated a radiocarbon date for individual BOO004, whose genome was shotgun
184 sequenced to 31.8x coverage (Table 1). The radiocarbon date (MAMS-57646) for this
185 individual was determined to be 3351±25 BP, or 1735-1538 calBC (± 2σ) after calibration with
186 OxCal 4.4²². However, we did not correct for a potential freshwater reservoir effect, which may
187 place BOO004 at a younger date.

188

189 **General population genetic results.** We used smartPCA²³ to perform a principal component
190 analysis (PCA) of modern-day reference populations from Eurasia and the Americas, onto
191 which the ROT and the BOO individuals were projected (Fig. 2a and b). When assessing the
192 genetic structure of Eurasian populations, plotting PC1 vs. PC2 (Fig. 2a) allows us to separate
193 west and east Eurasian populations from the Native American groups, while plotting PC1 vs
194 PC3 (Fig. 2b) distinguishes the major Eurasian ecological zones^{24,25}. Looking at the newly
195 generated data, ST individuals spread widely on the Eurasian PCA (PC1 vs PC3), mainly
196 throughout the so-called 'forest-tundra' genetic cline (Fig. 2b) mirroring the distribution of the
197 modern Uralic speakers (Supplementary Figure 4). Based on an unsupervised ADMIXTURE
198 analysis²⁶ of a reference set of published ancient data with K=7 clusters (Fig. 2c,
199 Supplementary Figure 5), the ROT individuals generally carry diverse ancestry components
200 ranging between a genetic profile represented by the Western Steppe Middle Late Bronze Age
201 cluster (Western_Steppe_MLBA, we use Sintashta_MLBA when modeling this ancestry going
202 forward)²⁷ - a combination of orange and dark and light blue colors - and that of the Late
203 Neolithic/Bronze Age East Siberians (Eastern_Siberia_LNBA)²⁸ - red color (Fig. 2c). In

204 comparison, the BOO individuals form a tighter and more homogeneous cluster that can be
 205 seen with both the PCA and the ADMIXTURE analyses, in line with what has been previously
 206 reported¹⁵.

207



208

209 **Figure 2.** (a) PCA results with ancient individuals projected onto modern variation calculated
 210 using modern Eurasian populations. Modern samples are shown in gray. Ancient reference
 211 individuals are listed under “Reference populations”, and the new individuals are listed under
 212 “New populations”. PC1 vs PC2 are plotted; (b) PCA results for PC1 vs PC3; (c) Unsupervised
 213 ADMIXTURE results with the relevant populations and sample names shown (k=7).

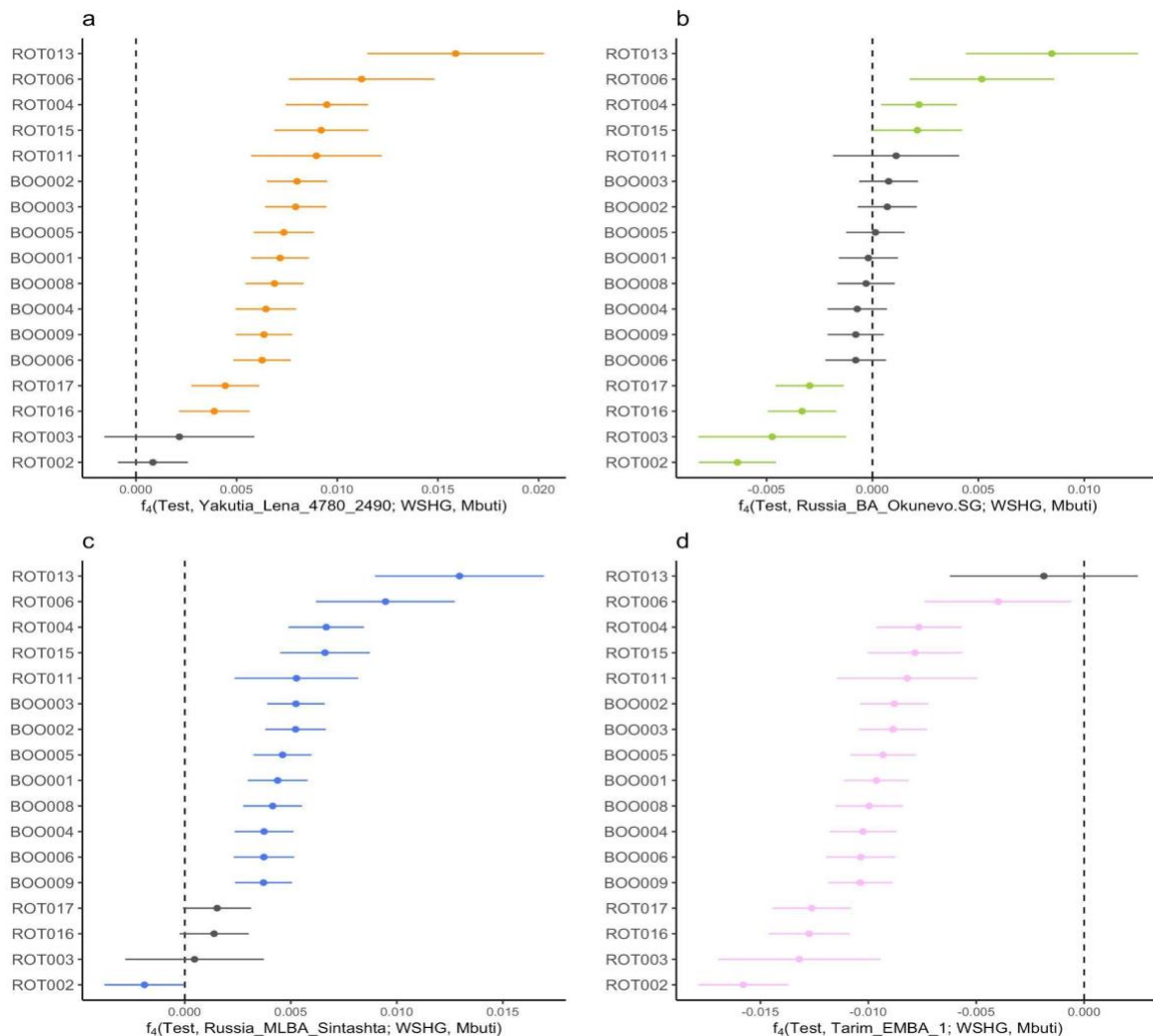
214

215

216 **F-statistics and qpAdm.** We calculated various F-statistics²⁹ to formally assess the
217 relationship of the ROT and BOO individuals with each other, and with different modern and
218 ancient reference individuals and populations. First, we performed outgroup f_3 -statistics of the
219 form $f_3(\text{Mbuti}; \text{test}, \text{modern})$ to test for the affinity of each ROT and BOO individual with modern
220 Eurasian populations (Supplementary Figure 6, Supplementary Table 2). The f_3 -statistics
221 results mirrored the distribution of the samples in the PCA and ADMIXTURE analyses, wherein
222 the individuals with higher proportions of Eastern_Siberia_LNBA ancestry (e.g. ROT002)
223 showed a greater affinity to the modern-day Siberian and Uralic-speaking populations, such
224 as Nganasan, Evenk, Negidal, Nanai, and Ulchi (Supplementary Figure 6A), whereas the
225 individuals with more Sintashta-like Western_Steppe_MLBA ancestry (e.g. ROT003) were
226 closer to modern-day (North) Europeans, including Norwegian, Belarusian, Lithuanian,
227 Scottish and Icelandic individuals (Supplementary Figure 6B). Comparisons with ancient
228 groups using $f_3(\text{Mbuti}; \text{test}, \text{published ancient})$ showed a similar trend (Supplementary Figure
229 6). For example, ROT002 on the ‘eastern end’ of the Eurasian cline, had the highest observed
230 f_3 -values, i.e. shared more genetic drift, with Eastern_Siberia_LNBA, Russia Ust Belaya
231 Neolithic, and Mongolia Early Iron Age individuals (Supplementary Figure 6A). By contrast,
232 ROT003, the ‘westernmost’ individual in the Eurasian PCA space, had the highest affinity with
233 Lithuania early Middle Neolithic Narva, Russia Sintashta, Kazakhstan Georgievsky Middle
234 Bronze Age, Russia Poltavka, and Serbia Mesolithic individuals (Supplementary Figure 6B).
235 Similar trends could be observed for the BOO, wherein the modern Uralic-speaking
236 populations, such as Nganasan and Selkup, were among the models with the highest f_3 -
237 statistics. Among the ancient f_3 comparisons, the most closely related individuals to BOO were
238 the Eastern European and West-Siberian hunter-gatherers (EEHG and WSHG), published
239 BOO, and Botai Eneolithic individuals from Kazakhstan (Supplementary Figures 6J and K).

240
241 Based on the geographic location of the sites, the results of the outgroup f_3 -statistics, and the
242 distribution of the ROT and BOO individuals on the PCA, we tested whether these individuals
243 retained more local Ancient North Eurasian (ANE) ancestry compared to contemporaneous
244 groups and individuals from the general region. To assess the genetic affinities of ROT and
245 BOO to known populations from similar general geographic area, time period, and
246 archaeological affiliation, we calculated f_4 -statistics of the form $f_4(X, \text{test}, \text{WSHG}, \text{Mbuti})$ where
247 X stood for ROT and BOO individuals, and *test* populations included Okunevo,
248 Tarim_EMBA_1, Sintashta_MLBA, and Eastern_Siberia_LNBA (Fig. 3). This test allowed us
249 to identify groups that are cladal with ROT and BOO (i.e., equidistantly related to WSHG), and
250 cases where ROT and BOO may have additional affinity to ANE (represented here by WSHG
251 from Tyumen oblast, Russia as the best spatial and temporal proxy). Based on the f_4 -statistics,
252 we find that ROT and BOO individuals carry excess affinity to ANE when compared to

253 Eastern_Siberia_LNBA (Fig. 3A) and Russia MLBA Sintashta (Fig. 3C), except for ROT002
 254 and ROT003. All BOO individuals are symmetrically related with the Okunevo Bronze Age
 255 group indicating no additional affinity to ANE (Fig. 3B). However, we see more heterogeneity
 256 in ROT, with some individuals having significantly more, and others significantly less genetic
 257 affinity to WSHG compared to Okunevo (Fig. 3B). All but one individual (ROT013) have
 258 significantly less ANE ancestry compared to Tarim EMBA (Fig. 3D). The general observations
 259 from f_4 -statistics mirror the trends we see in the PCA, especially when PC1 is plotted against
 260 PC2, wherein ROT individuals vary with regards to their location on the ANE cline represented
 261 by Afontova Gora 3 and Mal'ta 1, while the BOO individuals are more homogeneous (Fig. 2B).
 262



263
 264 **Figure 3. f_4 -statistics testing for excess ANE ancestry in ROT and BOO individuals.**
 265 Testing for excess ANE ancestry with respect to: (a) Yakutia Lena 4780-2490, (b) Okunevo,
 266 (c) Russia MLBA Sintashta, (d) Tarim EMBA1. Significantly non-zero f_4 -statistics ($|Z| > 3$) are
 267 shown in color, and non-significant f_4 -statistics are shown in gray. All error bars indicate 3
 268 standard errors. “Test” denotes the individuals given on the y-axis.

269

270 The cultural affiliation of the BOO individuals remains poorly understood. Based on the
271 archaeological information, such as the presence of 'Waffle' ware ceramics that are similar to
272 the Neolithic pottery from Yakutia and Chukotka¹⁶, it was hypothesized that the BOO
273 individuals represent a westward migration of Siberian populations along the forest-tundra and
274 forest-steppe zones. However, potential contacts with Scandinavian archaeological cultures,
275 such as Vardøy Ware, have been proposed for BOO¹⁶. To test this, we calculated pairwise f_3 -
276 statistics with different ancient populations from Scandinavia, which separated the BOO
277 individuals, as well the ROT from the rest of the populations ranging between Mesolithic to
278 Medieval time periods (Supplementary Figure 7). Together, these results suggest a non-local
279 genetic origin for the BOO individuals, and no substantial levels of early farmer ancestry,
280 consistent with PCA and admixture analyses.

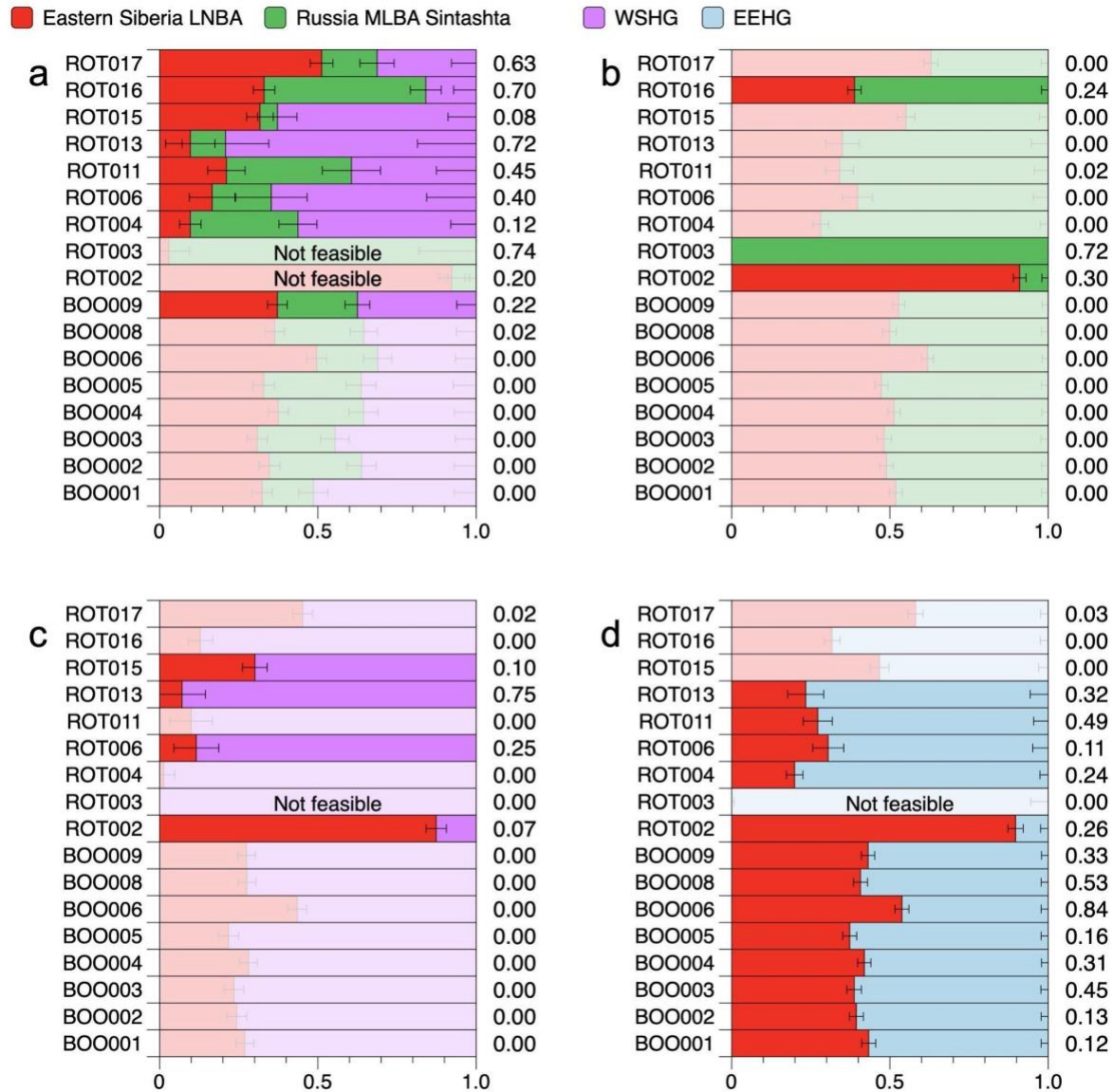
281

282 Lastly, we performed qpAdm analysis to formally test for and quantify the admixture
283 proportions in ROT and BOO individuals that we had identified in the previous analyses (Fig.
284 4, Supplementary Table 3). Here, we could successfully model the ROT individuals as a mix
285 of three ancestries, Eastern_Siberia_LNBA, Sintashta_MLBA, and WSHG, except for
286 ROT002, which could be modeled instead as a two-source mixture of mainly
287 Eastern_Siberia_LNBA ancestry and a smaller proportion of EEHG-like ancestry that could be
288 represented by either Sintashta_MLBA, WSHG, or EEHG, whereas ROT003 could be
289 modeled with Sintashta_MLBA as single source (Fig. 4B). We also tested whether ROT
290 individuals could be modeled as a two-way mixture of the Eastern_Siberia_LNBA ancestry and
291 either Sintashta_MLBA or WSHG as sources, however, this combination of ancestries did not
292 result in consistently plausible model fits, compared to the combination of all three ancestries
293 (Fig. 4a-c). By contrast, BOO individuals could not be modeled using either the combination of
294 all three ancestry sources (Eastern_Siberia_LNBA, Sintashta_MLBA, and WSHG), or just a
295 two-way mixture (Fig. 4a and c, Supplementary Table 3). However, replacing WSHG with
296 EEHG as the putative local hunter-gatherer ancestry stratum and using
297 Eastern_Siberia_LNBA as a second source provided good model fits (Fig. 4D, Supplementary
298 Table 4).

299

300 We then estimated the date of the admixture event in BOO individuals between the EEHG and
301 Eastern_Siberia_LNBA sources using DATES v.753³⁰. The admixture date was estimated to
302 be 17.98 ± 1.06 generations ago, or around 500 calendar years prior to the mean radiocarbon
303 date of BOO, assuming a generation time of 29 years³¹ (Supplementary Figure 8).

304



305

306 **Figure 4. Ancestry modeling results for ROT and BOO individuals.** (a) qpAdm models
 307 using Eastern Siberia LNBA, Russia MLBA Sintashta, and WSHG as sources; (b) qpAdm
 308 models with Eastern Siberia LNBA and Sintashta as sources; (c) qpAdm models with Eastern
 309 Siberia LNBA and WSHG as sources; (d) qpAdm models with Eastern Siberia LNBA and
 310 EEHG as sources. Corresponding p-values for each analysis are shown to the right of each
 311 row. Models with p-values < 0.05 are grayed out, and the models with negative ancestry
 312 proportions are indicated as “Not feasible”.

313

314 **Identity-by-descent (IBD) analysis.** We were interested in investigating distant biological
 315 relatedness among the BOO individuals (ROT individuals are below the required coverage
 316 threshold for imputation). To do so, we first imputed the genomes of the BOO individuals using
 317 GLIMPSE³² with the 1000G dataset³³ as a reference panel. Based on the identification of
 318 haplotype blocks of certain lengths that are shared between individuals, i.e. identical by

319 descent³⁴, we confirmed the 2nd degree related pair identified with READ (BOO004-BOO005),
320 we also found two 3rd degree related pairs (BOO003-BOO004 and BOO003-BOO005), as well
321 as multiple potential 4th/5th-degree related pairs. The fact that the BOO individuals are distantly
322 related to each other explains the relative homogeneity seen in the sample compared to ROT.
323 With regards to the archaeological data from these individuals, two pairs of biologically related
324 individuals were buried in the same graves, one 4th/5th-degree related pair: BOO005 (burial 17,
325 sepulture 3, female) and BOO009 (burial 17, sepulture 4, female), and one 3rd-degree related
326 pair: BOO003 (burial 16, sepulture 1, female) and BOO004 (burial 16, sepulture 3, male)¹⁶.

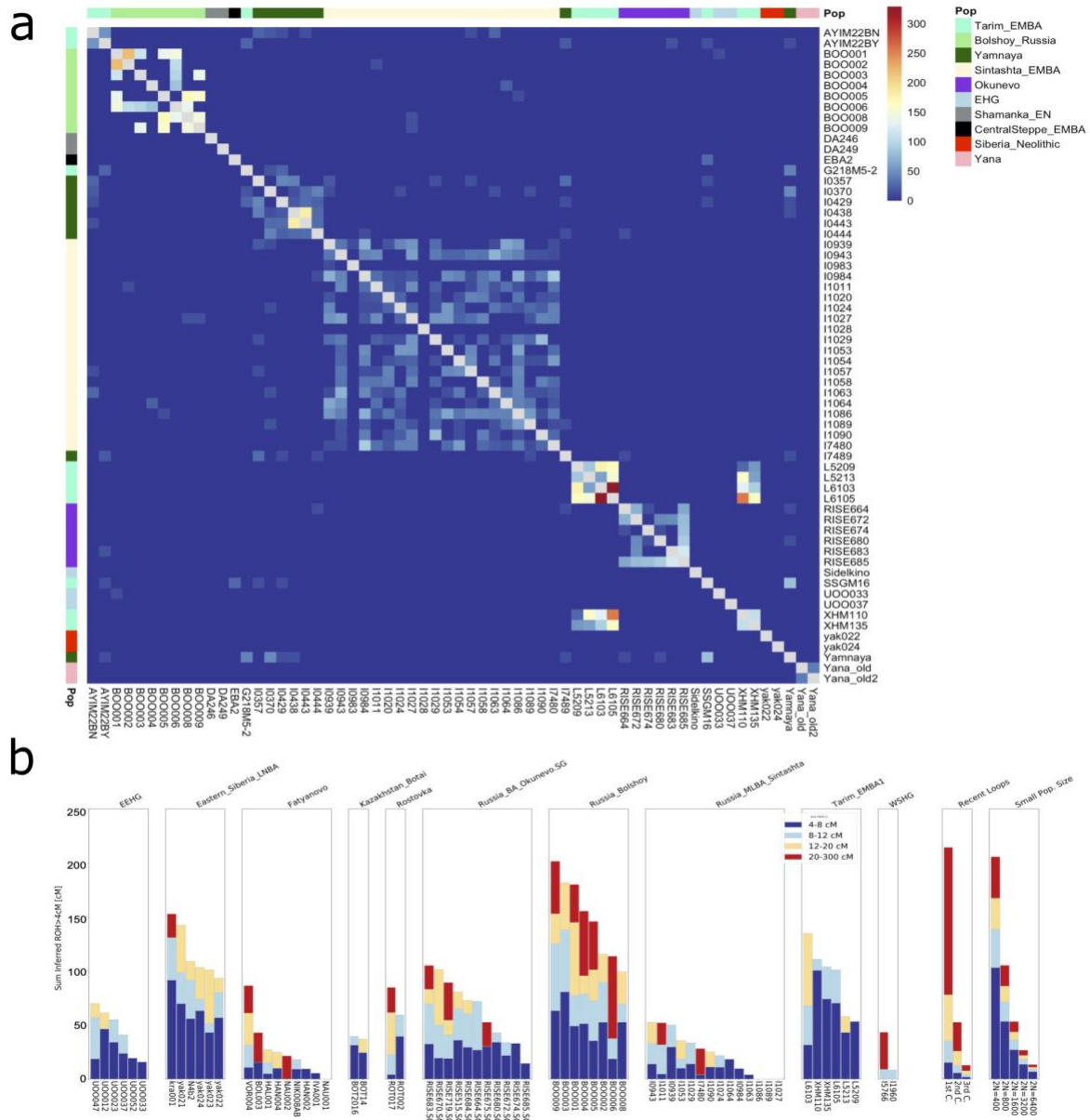
327

328 We also looked at IBD sharing between BOO and previously published individuals from groups
329 that are broadly contemporaneous chronologically and close geographically, including
330 Tarim_EMBA³⁵, Okunevo³⁶, Sintashta_MLBA²⁷, EEHG³⁷, Botai³⁶, Yamnaya³⁶,
331 Easter_Siberia_LNBA²⁸, and others (Fig. 5a, Supplementary Table 5). We found three shared
332 IBD fragments (14-22cM) between BOO individuals and Sintashta_MLBA individuals
333 (Supplementary Table 5), potentially suggesting shared ancestors as recent as approximately
334 500-750 years, and most likely reflecting the shared EEHG ancestry that is present in both
335 groups.

336

337 Runs of homozygosity. To get a sense of the underlying population structure, general
338 relatedness, and effective population sizes, we used HapROH to analyze runs-of-
339 homozygosity (ROH) in the genomes of the BOO individuals, together with already published
340 individuals with more than 400k SNPs on the 1240k SNP set³⁸. We compared BOO to
341 geographically and genetically close populations from the Eurasian forest steppe area,
342 including Okunevo, Sintashta_MLBA, EEHG (UOO), Eastern_Siberia_LNBA, Tarim EMBA,
343 and Fatyanovo (Fig. 5b). We also included two ROT individuals with more than 200K SNPs,
344 but their results should be interpreted with caution. The ROH analysis of BOO suggests that
345 this early Metal Age population had a relatively small effective population size of $\sim 2N=800$,
346 and one of the individuals (BOO006) appears to be an offspring of 2nd cousins. Tarim EMBA,
347 Okunevo, and Eastern_Siberia_LNBA groups also seemed to have relatively small effective
348 population sizes, while Fatyanovo and Sintashta potentially had larger effective population
349 sizes (Fig. 5b). In comparison, ROT individuals show similar ROH profiles to the populations
350 they are closely related to, based on the PCA and F-statistics, i.e., ROT002 resembles the
351 Eastern Siberian LNBA, and ROT017 – BOO (Fig. 5b).

352



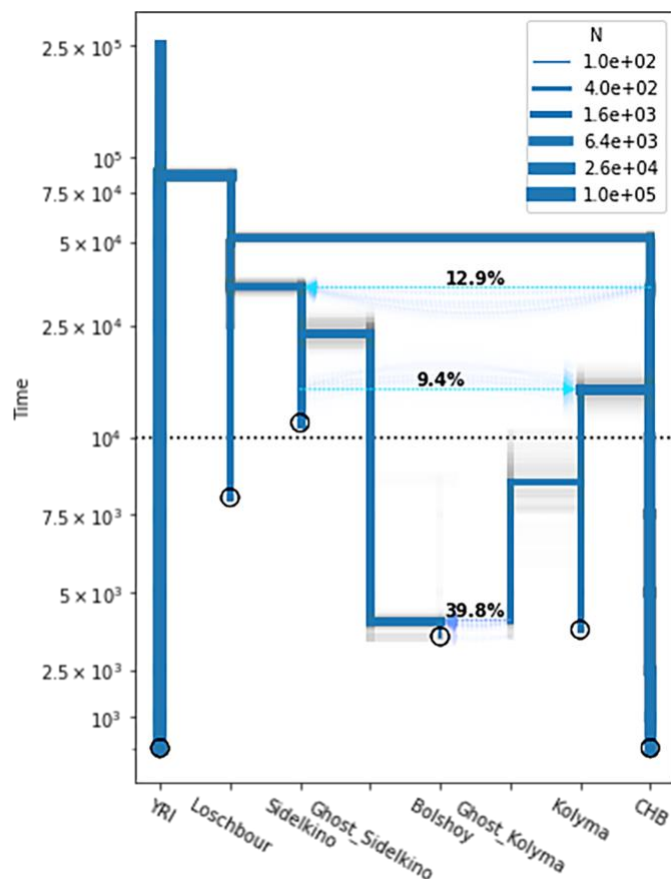
353
 354 **Figure 5.** (a) IBD sharing between BOO and published data. Shared IBD chunks between 12
 355 and 30 cM are shown. The total IBD length shared is indicated by the color of the square, and
 356 population designation is shown on the y-axis. (b) HapROH output for BOO, ROT and relevant
 357 contemporaneous populations. Runs of homozygosity (ROH) are plotted by population for
 358 individuals with more than 400k SNPs on the 1240k capture. ROH segments are colored
 359 according to their binned lengths.

360
 361

362 **Demographic modeling.** High-coverage shotgun data from BOO004 (~30x) allowed us to
 363 perform demographic modeling to investigate North Eurasian genetic ancestry and the nature
 364 of the admixture of the Eastern and Western Eurasian sources found in BOO individuals using
 365 a site-frequency spectrum (SFS) modeling-based method called momi2³⁹. We included

366 published data from representative North Eurasian populations, both preceding and
367 contemporaneous to BOO. After an incremental build-up of our model and including three
368 admixture events, our final model indicates a recent admixture for BOO individuals (95%
369 confidence interval (CI) 3596-4429 years ago), with substantial gene flow (39.9%; 95% CI
370 34.0-44.8%) from Eastern Eurasians (represented here by Late Neolithic/Bronze Age Siberian
371 individuals), which is consistent with the results from qpAdm. The population size estimated
372 for BOO (N=190, 95% CI 6-482) from momi2 (Fig. 6, Supplementary Table 6) is smaller than
373 the estimate obtained from hapROH (2N between 400 and 800 individuals, Fig. 6). This could
374 be explained by momi2 not taking into account inbreeding via the analysis of the runs of
375 homozygosity, and thus producing a biased estimate of the true effective population size. Thus,
376 we believe that the results produced by hapROH are closer to the true value of the effective
377 population size.

378



379

380 **Figure 6.** Momi2 demographic model for BOO004 using shotgun sequencing data from
381 published ancient and modern individuals. Point estimates of the final model are shown in blue;
382 results for 100 nonparametric bootstraps are shown in gray. The sampling times of populations
383 are indicated by circles. The population sizes are indicated by the thickness of branches. The
384 y-axis is linear below 10,000 years ago, and logarithmic above it. See Supplementary Table 6
385 for specific parameter values. YRI, Yoruba; CHB, Han Chinese.

386

387 **Y-chromosome haplogroups.** We performed Y-haplogroup (Y-hg) typing of the ROT males
388 using the YMCA method¹⁹ (Table 1). We identified two individuals that carried the R1a Y-hg
389 (ROT003 (R1a-M417) and ROT016 (R1a-Z645)), one of the most widely distributed Y-hgs in
390 Eurasia⁴⁰. However, both individuals could be R1a-Z645, since ROT003 does not have either
391 ancestral or derived ISOGG list SNPs after R1a-M417. The earliest evidence for Y-hg R1a
392 comes from Mesolithic EEHG individuals^{41,42}, and it is widespread throughout Eurasia today,
393 from Scandinavia to South Asia and Siberia⁴⁰. Specifically, R1a-M417 is common among
394 Corded Ware-associated individuals^{41,43}, while the derived R1a-Z645 is common in the Baltic
395 Corded Ware⁴⁴ and Fatyanovo¹³. Generally, due to their geographic distribution, these R1a
396 haplogroups are thought to represent the eastward movement of the Corded Ware-, and
397 Fatyanovo-associated groups.

398 ROT002, the individual with the highest proportion of north Siberian ancestry, was assigned to
399 the N1a1a1a1a (N-L392) haplogroup. This Y-hg has also been found in two published BOO
400 individuals¹⁵. The lineage N-L392 is one of the most common in present-day Uralic
401 populations, and was estimated to have split from other N-lineages around 4,995 years ago⁴⁵.
402 This finding further highlights the importance of Y-hg N-L392 as being linked to the
403 dissemination of proto-Uralic, but potentially also involving the ST network.

404 One of the males (ROT004) was assigned to haplogroup Q1b (Q-M346), which is found
405 throughout Asia, including in several Turkic speaking populations, i.e. Tuvians, Todjins,
406 Altaians, Sojots, etc., and Mongolian-speaking Kalmyk population⁴⁶. Another individual
407 (ROT017) was determined to belong to the Q1b1 (Q-L53) haplogroup, which is common
408 among present-day Turkic speakers across Eurasia. The branch Q-YP4004 includes Central
409 Asian Q-L53(xL54) lineages and one ancient Native American individual from Lovelock Cave
410 in Nevada dated 1.8 ky⁴⁷, and the oldest individual with this haplogroup is irk040 (Cis-Baikal
411 Neolithic, 4846 BP)²⁸. The lineage C2a-L1373, carried by ROT011, is found at high frequency
412 in Central Asian populations, North Asia and the Americas. C2a-L1373 expanded to North Asia
413 and the Americas post-LGM, around 17,700–14,300 years ago⁴⁸. Lastly, haplogroup R1b1a1a
414 (R1b-M73), a sister-clade of R1b-M269, is carried by ROT006. This lineage is common in the
415 Caucasus, Siberia, Mongolia, and Central Asia today⁴⁶.

416 Overall, the Y-hg lineage diversity of male ROT individuals further highlights the
417 heterogeneous nature of the ST, which has also been proposed by archaeologists⁴⁹.

418

419 **Mitochondrial haplogroups.** We identified a large diversity in the mitochondrial haplogroups
420 (mt-hg) among ROT (Table 1), including mt-hgs that are found commonly in east Eurasia (A10,
421 C1, C4, G2a1)^{50–53} and in west Eurasia (H1, H101, U5a, R1b, R1a)^{36,54}, and similar to the
422 trends seen from autosomal and Y-hg point of view. For example, the individual ROT002 with

423 the highest affinity to Siberia_LNBA and carrying the Y-hg N-L392 also carries a mt-hg G2a1
424 commonly found in Eastern Eurasia. On the other hand, the individual ROT003 with the highest
425 affinity to Sintashta_MLBA and carrying the Corded-ware derived Y-hg R1a1a1, is also a
426 carrier of the R1a1a mt-hg commonly found in west Eurasia.

427

428 **Discussion**

429

430 Metallurgical production is an important human cultural innovation that has been developed
431 multiple times in multiple locations around the globe, one of which is Bronze Age Eurasia. It is
432 during the Bronze Age period that the Seima-Turbino transcultural phenomenon is identified
433 based on the evidence of skilled metallurgical production which is visible in the archaeological
434 record of Northern Eurasia. The ST phenomenon holds an important place in the development
435 of metallurgy within the framework of the Bronze Age Northern Eurasia, as the distribution of
436 knowledge about the usage of Sn is one of its core elements⁴.

437

438 This study is reporting genome-wide data of ST-associated individuals and their connections
439 to individuals associated with contemporaneous and preceding archaeological groups of the
440 northern Eurasian forest-steppe and steppe during the Bronze Age, such as Sintashta,
441 Okunevo, as well as Neolithic and Bronze Age Siberian groups. We also reassess the genetic
442 structure of BOO individuals of northwestern Russia that have been shown to carry high levels
443 of Siberian ancestry, an important characteristic of northern Eurasia.

444

445 The observed genetic heterogeneity among the ROT individuals can either suggest a group at
446 an early stage of admixture, or signify the heterogeneous nature of the ST complex⁴. Together
447 with evidence from the available archaeological data⁴, we argue that the individuals buried at
448 ROT more likely represent a variety of genetic and perhaps cultural backgrounds, brought
449 together by the ST metallurgical network. The findings from genome-wide autosomal data in
450 PCA, ADMIXTURE and F-statistics are mirrored in the Y-chromosomal and mitochondrial data.
451 Eight males of nine ROT individuals represent both eastern Eurasian and Western Eurasian
452 Y-chromosomal lineages, and eastern and western Eurasian mitochondrial lineages,
453 respectively, further highlighting the genetic heterogeneity seen in ROT. In general, the region
454 of the Middle Irtysh around Rostovka can be characterized as the typological melting pot of
455 the western and eastern part of the ST phenomenon mirroring in the genetic data.

456

457 On an individual level, there is no clear correlation between genetic ancestry of the screened
458 individuals and the cultural/regional attribution of their grave goods. The inventory of the burial
459 of individual ROT003 with western Eurasian genetic ancestry includes artifacts, which can be

460 attributed to the eastern part of the ST phenomenon (forked lancehead with hook, trapezoidal
461 socket axe) and there are regionally nonspecific ST-artifacts (lamellar dagger blades, forked
462 lancehead with two loops), as well as ceramics of the Krotovo and Okunevo cultures. Artifacts
463 with a connection to the Steppe-related cultures of the Transurals or the western part of the
464 ST phenomenon are not present. The rather sparse burial of ROT002 does not stand out
465 typologically in contrast to most other burials of the cemetery, despite the genetic attribution to
466 the Eastern Siberian LNBA^{4,55}.

467

468 In case of BOO, we see a very homogeneous genetic profile that we can model as a recent
469 mixture of the Neolithic Siberian and EEHG components approximately ~2200-2000 BCE,
470 which places this event at a similar time as the temporal peak of the ST phenomenon.
471 Interestingly, despite the geographic location of the burial site on the Kola Peninsula in
472 northwestern Russia, BOO individuals carry higher proportions of 'eastern' Siberian ancestry
473 than most ROT individuals. The genetic homogeneity observed in BOO individuals can be
474 explained by the genetic background relatedness as shown by IBD sharing and ROH analysis,
475 which is indicative of a relatively small or isolated population.

476 We also find that BOO and ROT exhibit distinct genetic subtleties with regard to the presence
477 of the Early European Farmer ancestry. Although relatively contemporaneous, ROT
478 individuals, in general, carry higher levels of Neolithic farmer-related ancestry, which we were
479 able to model as part of the Sintashta_MLBA in our admixture models. However, this ancestry
480 is not present in BOO individuals, which carry HG-related ancestry that is more similar to a
481 more ancient, but local EEHG stratum (as demonstrated for the nearby Yuzhny Oleni Ostrov
482 site)^{41,56}. The lack of European farmer ancestry in BOO, contrary to what has been reported in
483 Lamnidis 2018 (Figure 4a), also highlights the natural limits of the farming subsistence practice
484 and the spread of farmer-related ancestry mediated by MBA forest steppe pastoralists into the
485 northernmost parts of Eurasia during this time period.

486

487 We tested the individuals in this study with regards to the presence of Ancient North Eurasian
488 ancestry, also known as the Upper Paleolithic Siberian ancestry that was first described in
489 individuals from Mal'ta and Afontova Gora 2 and 3^{56,57}, and marks a basal North Eurasian
490 lineage that is shared between modern-day Europeans and Native Americans, but not found
491 in southern India, East and Southeast Asia. This ancestry is generally associated with groups
492 falling on the forest tundra genetic cline²⁵, and is present in high levels in the Bronze Age Tarim
493 mummies³⁵. We found that the ST individuals vary with regards to their location on the ANE
494 cline towards Afontova Gora 3 and Mal'ta 1, in line with the findings from PCA and
495 ADMIXTURE analyses. BOO individuals also carry the ANE ancestry, but in a more
496 homogeneous fashion.

497

498 With the new data from ROT, we are able to assess a recent proposal which suggested that
499 Uralic languages could have been used within the ST network leading to the initial spread of
500 Uralic languages across the Eurasian forest steppe^{58–60}. After performing various tests of
501 genetic structure of the ST-associated individuals, we report genetic profiles on an ancestry
502 cline that generally mirrors the genetic distribution of modern-day Uralic-speaking populations
503 of the northernmost forest-tundra (taiga and tundra) ecological cline²⁵. Our findings show that
504 the ST-associated individuals from Rostovka likely did not originate from a single location but
505 rather represent people from a wide geographical area. Seima-Turbino was a latitudinal
506 phenomenon on the same east-west axis where also the hypothetical homelands of the
507 ancestral Uralic subgroups were positioned⁶¹. Thus, our genetic results are temporally and
508 geographically consistent with the proposal that Uralic languages could have spread within the
509 ST network, but are neither a clear nor a direct proof. Further ancient human DNA data from
510 northern Eurasia will help elucidate the details of the wider spread of ancient Siberian ancestry
511 and its association with proto-Uralic speaking groups.

512

513 Taken together, our findings show that all but one of the carriers of artifacts associated with
514 the ST transcultural phenomenon have genetic similarities to the current taiga-tundra area
515 populations, but harbor an extremely diverse mix of western and eastern Eurasian ancestries.
516 However, due to the limited number of individuals studied, we cannot be certain as to what
517 degree the individuals in this study represent the ST phenomenon as a whole. Genetic data
518 from other confidently ST-associated sites will be crucial in providing a comparative analysis
519 of the data. Lastly, we investigate the genetic history of the Siberian ancestry in northern
520 Eurasia, and suggest that there were possibly several waves of migration of people carrying
521 the Siberian ancestry component, indicating a complex demographic history of the region.

522

523 **Materials and Methods**

524

525 **Archaeological background.** Rostovka (ROT) is a ST burial site located on the river Om, in
526 the city of Omsk, and was excavated in 1966-1969⁹. A total of 38 graves were excavated at
527 the site, not all of which contained human remains. Some of the individuals buried at Rostovka
528 were cremated, including ten clear cases of cremation, two graves with charcoal only, and one
529 case with charcoal and the remains of children⁵⁵.

530

531 The burial ground of Rostovka occupies a very curious position within the ST phenomenon. It
532 is the largest ST-site east of the foothills of the Ural Mountains. It is, compared to other
533 important sites like Seima and Turbino, well excavated, documented and published. Rostovka

534 is, together with the smaller sites of Kargat 6 and Preobrazhenka 6, the most eastern point of
535 the distribution of steppe-related artifacts in ST-contexts. At these three sites also specifically
536 western ST-artifacts still appear, but in very small numbers. The ceramics of Rostovka are
537 connected to the Krotovo and other forest-steppe cultures. The stone-artifacts are partly
538 connected to the traditions of Baikalian stone-tools (little arrowheads, rectangular blades)
539 partly to the western part of the ST phenomenon (bigger arrowheads, irregular blades) and in
540 the case of a stone mace head to the Steppe-related cultures of the Transurals⁵⁵. The metal
541 composition of the artifacts of Rostovka is very comparable to the overall tendencies of the ST
542 phenomenon. Steppe-related artifacts tend to contain less Sn than regional nonspecific ST-
543 artifacts. And these nonspecific ST-artifacts contain less Sn than eastern ST-artifacts.

544

545 A total of 19 individuals from Rostovka were screened for ancient DNA preservation using
546 shotgun sequencing of 5M reads, however, only nine passed the 0.1% endogenous DNA cutoff
547 to be further analyzed using capture arrays. The low success rate is explained by the fact that
548 the macroscopic preservation of the skeletal remains was poor in general, and we could only
549 sample random parts of long bones and few teeth, but no petrous bones

550

551 BOO was first excavated in 1925, with the most recent excavation taking place between 2001-
552 2004¹⁶. A total of N=43 individuals were found, along with wooden grave constructions, as well
553 as bone, antler, stone, ceramic, and bronze items. Most burials were inhumations, with the
554 exception of three cremations, and most individuals were buried in wooden boat-shaped
555 caskets¹⁶.

556

557 **DNA extraction and data generation.** All aDNA work was done in dedicated clean laboratory
558 facilities following the standard protocols⁶². Briefly, single-stranded libraries were produced for
559 ROT, and double-stranded UDG-half libraries were produced for the new BOO individuals.
560 First, shotgun libraries were screened for the presence of endogenous DNA, and samples with
561 the aDNA content above 0.1% were captured for the 1240k sites. We also produced mtDNA
562 and Y-haplogroup capture data for the samples included in the study. A set of BOO individuals
563 were shotgun sequenced to high coverage. The nfcere/eager pipeline v.2.3.5⁶³ was used to
564 process the samples from fastq files to the deduplicated bam files. The software version
565 information is listed in Supplementary Table 7. Briefly, samples were mapped to the hs37d5
566 version of the human reference genome using bwa aln with the following parameters: bwa aln
567 -o 3 -n 0.001 -l 16500. Pseudohaploid genotyping calls for the ROT individuals were produced
568 using pileupcaller (<https://github.com/stschiff/sequenceTools>) with the --singlestrandmode
569 option. We trimmed two base pairs from bam files of BOO individuals from each side of the
570 read, and genotyped the samples to produce pseudohaploid calls with pileupcaller

571 (<https://github.com/stschiff/sequenceTools>). The ancient DNA status of the samples was
572 authenticated using MapDamage v2⁶⁴. Contamination from modern sources was determined
573 using a combination of contammix⁶⁵, schmutzi⁶⁶, ANGSD X-chromosome contamination
574 estimate (for males)⁶⁷, and sex determination. READ²⁰ and pairwise mismatch rate (PMR)
575 were used to perform biological relatedness analysis. PMRs were calculated from
576 pseudohaploid genotypes of the 1240k panel.

577

578 **Population genetics analyses.** The projection PCA was done using smartpca²³ including
579 already published ancient and modern data from the Allen Ancient DNA Resource (AADR)
580 v44.3⁶⁸ using the projection mode, wherein ancient samples were projected upon modern
581 genetic variation. Unsupervised admixture analysis was done on the ROT and the new BOO
582 data together with already published ancient DNA samples from the AADR v44.3⁶⁸ using
583 ADMIXTURE²⁶ for 1-20 K clusters between in 5 iterations. Coefficients of variance for each K
584 were compared and the best K level was chosen based on the lowest average CV.

585

586 The f-statistics and qpAdm analyses were performed using admixr⁶⁹. The resulting data were
587 plotted using DataGraph v.4.6.1, and R⁷⁰ using the ggplot2 package⁷¹. For qpAdm, we used
588 Mbuti, Georgia_Kotias.SG, Israel_Natufian_published, Ami, Mixe, Italy_North_Villabruna_HG,
589 and ONG.SG as an outgroup set (based on¹⁵).

590

591 Mitochondrial haplogroups were determined using HaploGrep2⁷² using the data from the
592 mitochondrial capture. Briefly, mitochondrial capture data was mapped to the mitochondrial
593 reference genome NC_012920.1 using circularmapper⁷³ and mapping quality threshold of 30.
594 Bam files were then imported into Geneios and a consensus fasta file was produced with the
595 coverage threshold of 5, and Sanger heterozygotes set to >50%. The consensus fasta file was
596 then imported into HaploGrep2. Y-haplogroup data generated using YMCA was used to assign
597 Y-chromosome haplogroups to male ROT individuals following the method described in¹⁹.

598

599 ROH analysis was done using HapROH³⁸ on the pseudohaploid data from BOO, together with
600 already published individuals, and only focusing on samples with more than 400k SNPs from
601 the 1240k SNP array.

602

603 BOO samples were imputed and phased using GLIMPSE³² following the default parameters,
604 and merged with already published data, in order to test for patterns of IBD sharing among the
605 individuals using ancIBD³⁴. IBD analyses were restricted to samples covering more than 600K
606 SNPs with GP>=0.99 after genotype imputation. IBD results were plotted using the R package
607 pheatmap⁷⁴.

608

609 **Demographic modeling.** We used DATES³⁰ to determine the time of admixture in BOO using
610 Yakutia_Lena and UOO as the two reference sources. Demographic modeling of BOO was
611 then performed using momi2³⁹. To do so, we added several already published samples into
612 our model to give sufficient background information: two random individuals from YRI (Yoruba
613 in Ibadan, Nigeria) in 1000 Genomes Project³³ representing the Africans; two random
614 individuals from CHB (Han Chinese in Beijing, China) in 1000 Genomes Project representing
615 East Asians; the 8000-year-old Loschbour individual from Luxembourg⁷⁵ representing WEHG;
616 one Mesolithic individual from Sidelkino, Russia⁷⁶ representing EEHG; two Late
617 Neolithic/Bronze Age individuals from Kolyma river regions of Yakutia, Russia²⁸ representing
618 the Eastern Siberia LNBA. Ancient samples were downloaded from the European Nucleotide
619 Archive (ENA) as bam files, and then processed and imputed using GLIMPSE, following the
620 default parameters³². Modern individuals were extracted from the 1000G database³³. We
621 assumed a mutation rate of 1.25×10^{-8} per site per generation⁷⁷ and a generation time of 29
622 years³¹. We progressively added more populations into the model. For each step we randomly
623 initialized the new parameters dozens of times and did optimization respectively, and selected
624 the best model as the basis of the next step. The initial model involves Western Eurasians
625 (Loschbour) and Eastern Eurasians (CHB) as a simple split, with Africans (YRI) the outgroup.
626 Each lineage was modeled to have its own population size. We also defined the ancestral
627 Eurasian population size and the ancestral modern human size, and let the size of Loschbour
628 and CHB exponentially change from the ancestral Eurasian size. We then added the EEHG
629 (Sidelkino) lineage onto Loschbour, and Eastern Siberia LNBA (Kolyma) onto CHB, with their
630 own population sizes. The shared ANE ancestry in Sidelkino and Kolyma was modeled as
631 gene flow between Western and Eastern Eurasians. In actual modeling, we defined gene flow
632 from ancestral Eastern Eurasians to Sidelkino, as well as gene flow from Sidelkino to Kolyma.
633 At last, we added the highest coverage BOO individual BOO004 (Bolshoy) into the model, as
634 an admixture of Sidelkino and Kolyma. We finally defined the ghost lineage for two source
635 populations, with the same population size as their original branch, and modeled the Bolshoy
636 lineage as the admixture of ghost lineages. When optimizing the final model, we got a series
637 of similar likelihood results with recent admixture time and small population size in Bolshoy
638 Oleni Ostrov lineage. We chose the final model whose admixture time matches the conclusion
639 in DATES. To examine the stability of the parameters, we conducted 100 nonparametric
640 bootstraps, fit the model for each bootstrap dataset using the parameter values of the final
641 model as initial values, and computed the 95% confidence interval for each parameter. Each
642 bootstrap dataset was created by dividing the whole genome into 100 equal-sized blocks and
643 resampling the same number of blocks with replacement.

644

645 **Data Availability.** Genomic data (BAM and fastq formats) are available on the European
646 Nucleotide Archive (ENA) under accession number PRJEBXXX, genotypes in eigenstrat
647 format can be found at <https://edmond.mpdl.mpg.de>.

648

649 **Acknowledgments**

650

651 We would like to thank all members of the Department of Archaeogenetics at the Max Planck
652 Institute for Evolutionary Anthropology, the PALEoRIDER & Population Genetics Group. We
653 also thank Dr. Elina Salmela for her suggestions and comments, and Dr. Rüdiger Krause. This
654 work was funded by the European Research Council (ERC) under the European Union's
655 Horizon 2020 research and innovation program under grant agreement no. 771234-
656 PALEoRIDER (to W.H.). Kuzminykh S.V. was supported by the program from the Archaeology
657 Institute of the Russian Academy of Sciences No. NIOKTR 122022200264-9. Fabian Fricke
658 was funded through a DFG grant titled "Zur Metallurgie der bronzzeitlichen Artefakte des
659 Fundplatzes Sajtanska (nördlich von Ekaterinburg) vom Typ Sejmo-Turbino in Eurasien" (Dr.
660 Rüdiger Krause).

661

662

663 **References**

- 664 1. Chernykh, E. N. *Ancient Metallurgy in the USSR: The Early Metal Age*. (CUP Archive,
665 1992).
- 666 2. Kohl, P. L. *The Making of Bronze Age Eurasia*. (Cambridge University Press, 2007).
- 667 3. Hanks, B. K., Epimakhov, A. V. & Renfrew, A. C. Towards a refined chronology for the
668 Bronze Age of the southern Urals, Russia. *Antiquity* **81**, 353–367 (2007).
- 669 4. Chernykh, E. N. & Kuzminykh, S. V. Древняя металлургия Северной Евразии
670 (сейминско-турбинский феномен). <https://elibrary.ru/item.asp?id=21143678> (1989).
- 671 5. Linduff, K. M. Metallurgy in ancient eastern Eurasia. in *Encyclopaedia of the History of*
672 *Science, Technology, and Medicine in Non-Western Cultures* 3103–3116 (Springer
673 Netherlands, 2016).
- 674 6. Кузьминых, С. В. Сейминско-турбинская проблема: новые материалы. *Краткие*
675 *сообщения Института археологии* 240–263 (2011).
- 676 7. Korochkova, O. *Sacred Place of the First Metallurgists in the Middle Ural*.
677 (Издательство Уральского университета, 2020).
- 678 8. Parpola, A. Formation of the Indo-European and Uralic (Finno-Ugric) language families
679 in the light of archaeology: Revised and integrated “total” correlations.
680 https://researchportal.helsinki.fi/files/127256289/Parpola_A_2012._Formation_of_the_Indo_European_and_Uralic_language_families_in_the_light_of_archaeology._MSFOu_26
681

- 682 6.pdf (2012).
- 683 9. Marchenko, Z. V., Svyatko, S. V., Molodin, V. I., Grishin, A. E. & Rykun, M. P.
684 Radiocarbon Chronology of Complexes With Seima-Turbino Type Objects (Bronze Age)
685 in Southwestern Siberia. *Radiocarbon* **59**, 1381–1397 (2017).
- 686 10. Chernykh, E. N. *et al.* Issues in the calendar chronology of the seima-turbino
687 transcultural phenomenon. *Archaeol. Ethnol. Anthropol. Eurasia (Russ.-lang.)* **45**, 45–55
688 (2017).
- 689 11. Ковтун, И. В., Марочкин, А. Г. & Герман, П. В. Радиоуглеродные даты и
690 относительная хронология сейминско-турбинских, крохалёвских и самусьских
691 древностей. *Труды V (XXI) Всероссийского* (2017).
- 692 12. Tambets, K. *et al.* Genes reveal traces of common recent demographic history for most
693 of the Uralic-speaking populations. *Genome Biology* vol. 19 Preprint at
694 <https://doi.org/10.1186/s13059-018-1522-1> (2018).
- 695 13. Saag, L. *et al.* The Arrival of Siberian Ancestry Connecting the Eastern Baltic to Uralic
696 Speakers further East. *Curr. Biol.* **29**, 1701-1711.e16 (2019).
- 697 14. Der Sarkissian, C. *et al.* Ancient DNA reveals prehistoric gene-flow from siberia in the
698 complex human population history of North East Europe. *PLoS Genet.* **9**, e1003296
699 (2013).
- 700 15. Lamnidis, T. C. *et al.* Ancient Fennoscandian genomes reveal origin and spread of
701 Siberian ancestry in Europe. *Nat. Commun.* **9**, 5018 (2018).
- 702 16. Murashkin, Kolpakov & Shumkin. Kola Oleneostrovskiy grave field: a unique burial site
703 in the European Arctic. *Iskos* (2016).
- 704 17. Mathieson, I. *et al.* Genome-wide patterns of selection in 230 ancient Eurasians. *Nature*
705 **528**, 499–503 (2015).
- 706 18. Fu, Q. *et al.* An early modern human from Romania with a recent Neanderthal ancestor.
707 *Nature* **524**, 216–219 (2015).
- 708 19. Rohrlach, A. B. *et al.* Using Y-chromosome capture enrichment to resolve haplogroup
709 H2 shows new evidence for a two-path Neolithic expansion to Western Europe. *Sci.*
710 *Rep.* **11**, 15005 (2021).
- 711 20. Monroy Kuhn, J. M., Jakobsson, M. & Günther, T. Estimating genetic kin relationships in
712 prehistoric populations. *PLoS One* **13**, e0195491 (2018).
- 713 21. Lipatov, M., Sanjeev, K., Patro, R. & Veeramah, K. R. Maximum Likelihood Estimation of
714 Biological Relatedness from Low Coverage Sequencing Data. *bioRxiv* 023374 (2015)
715 doi:10.1101/023374.
- 716 22. Ramsey, C. B. Bayesian Analysis of Radiocarbon Dates. *Radiocarbon* **51**, 337–360
717 (2009).
- 718 23. Patterson, N., Price, A. L. & Reich, D. Population structure and eigenanalysis. *PLoS*

- 719 *Genet.* **2**, e190 (2006).
- 720 24. Wang, C.-C. *et al.* Ancient human genome-wide data from a 3000-year interval in the
721 Caucasus corresponds with eco-geographic regions. *Nat. Commun.* **10**, 1–13 (2019).
- 722 25. Jeong, C. *et al.* The genetic history of admixture across inner Eurasia. *Nat Ecol Evol* **3**,
723 966–976 (2019).
- 724 26. Alexander, D. H., Novembre, J. & Lange, K. Fast model-based estimation of ancestry in
725 unrelated individuals. *Genome Res.* **19**, 1655–1664 (2009).
- 726 27. Narasimhan, V. M. *et al.* The formation of human populations in South and Central Asia.
727 *Science* **365**, (2019).
- 728 28. Kılınc, G. M. *et al.* Human population dynamics and *Yersinia pestis* in ancient northeast
729 Asia. *Sci Adv* **7**, (2021).
- 730 29. Patterson, N. *et al.* Ancient admixture in human history. *Genetics* **192**, 1065–1093
731 (2012).
- 732 30. Chintalapati, M., Patterson, N. & Moorjani, P. Reconstructing the spatiotemporal
733 patterns of admixture during the European Holocene using a novel genomic dating
734 method. *bioRxiv* 2022.01.18.476710 (2022) doi:10.1101/2022.01.18.476710.
- 735 31. Fenner, J. N. Cross-cultural estimation of the human generation interval for use in
736 genetics-based population divergence studies. *Am. J. Phys. Anthropol.* **128**, 415–423
737 (2005).
- 738 32. Rubinacci, S., Ribeiro, D. M., Hofmeister, R. J. & Delaneau, O. Efficient phasing and
739 imputation of low-coverage sequencing data using large reference panels. *Nat. Genet.*
740 **53**, 120–126 (2021).
- 741 33. 1000 Genomes Project Consortium *et al.* A global reference for human genetic variation.
742 *Nature* **526**, 68–74 (2015).
- 743 34. Ringbauer, H. *et al.* ancIBD - Screening for identity by descent segments in human
744 ancient DNA. *bioRxiv* 2023.03.08.531671 (2023) doi:10.1101/2023.03.08.531671.
- 745 35. Zhang, F. *et al.* The genomic origins of the Bronze Age Tarim Basin mummies. *Nature*
746 **599**, 256–261 (2021).
- 747 36. de Barros Damgaard, P. *et al.* The first horse herders and the impact of early Bronze
748 Age steppe expansions into Asia. *Science* **360**, eaar7711 (2018).
- 749 37. Posth, C. *et al.* Palaeogenomics of upper Palaeolithic to neolithic European hunter-
750 gatherers. *Nature* **615**, 117–126 (2023).
- 751 38. Ringbauer, H., Novembre, J. & Steinrücken, M. Parental relatedness through time
752 revealed by runs of homozygosity in ancient DNA. *Nat. Commun.* **12**, 1–11 (2021).
- 753 39. Kamm, J., Terhorst, J., Durbin, R. & Song, Y. S. Efficiently inferring the demographic
754 history of many populations with allele count data. *J. Am. Stat. Assoc.* **115**, 1472–1487
755 (2020).

- 756 40. Underhill, P. A. *et al.* The phylogenetic and geographic structure of Y-chromosome
757 haplogroup R1a. *Eur. J. Hum. Genet.* **23**, 124–131 (2015).
- 758 41. Haak, W. *et al.* Massive migration from the steppe was a source for Indo-European
759 languages in Europe. *Nature* **522**, 207–211 (2015).
- 760 42. Saag, L. *et al.* Genetic ancestry changes in Stone to Bronze Age transition in the East
761 European plain. *Sci Adv* **7**, (2021).
- 762 43. Papac, L. *et al.* Dynamic changes in genomic and social structures in third millennium
763 BCE central Europe. *Sci Adv* **7**, (2021).
- 764 44. Saag, L. *et al.* Extensive Farming in Estonia Started through a Sex-Biased Migration
765 from the Steppe. *Curr. Biol.* **27**, 2185-2193.e6 (2017).
- 766 45. Ilumäe, A.-M. *et al.* Human Y Chromosome Haplogroup N: A Non-trivial Time-Resolved
767 Phylogeography that Cuts across Language Families. *Am. J. Hum. Genet.* **99**, 163–173
768 (2016).
- 769 46. Malyarchuk, B. *et al.* Ancient links between Siberians and Native Americans revealed by
770 subtyping the Y chromosome haplogroup Q1a. *J. Hum. Genet.* **56**, 583–588 (2011).
- 771 47. Grugni, V. *et al.* Analysis of the human Y-chromosome haplogroup Q characterizes
772 ancient population movements in Eurasia and the Americas. *BMC Biol.* **17**, 3 (2019).
- 773 48. Sun, J. *et al.* Post-last glacial maximum expansion of Y-chromosome haplogroup C2a-
774 L1373 in northern Asia and its implications for the origin of Native Americans. *Am. J.*
775 *Phys. Anthropol.* **174**, 363–374 (2021).
- 776 49. Molodin & Durakov. The adaptation of the Seima-Turbino tradition to the Bronze Age
777 cultures in the south of the West Siberian plain. *& Anthropology of*
- 778 50. Schurr, T. G., Sukernik, R. I., Starikovskaya, Y. B. & Wallace, D. C. Mitochondrial DNA
779 variation in Koryaks and Itel'men: population replacement in the Okhotsk Sea-Bering
780 Sea region during the Neolithic. *Am. J. Phys. Anthropol.* **108**, 1–39 (1999).
- 781 51. Volodko, N. V. *et al.* Mitochondrial genome diversity in arctic Siberians, with particular
782 reference to the evolutionary history of Beringia and Pleistocenic peopling of the
783 Americas. *Am. J. Hum. Genet.* **82**, 1084–1100 (2008).
- 784 52. Pilipenko, A. S., Trapezov, R. O., Zhuravlev, A. A., Molodin, V. I. & Romaschenko, A. G.
785 MtDNA Haplogroup A10 Lineages in Bronze Age Samples Suggest That Ancient
786 Autochthonous Human Groups Contributed to the Specificity of the Indigenous West
787 Siberian Population. *PLoS One* **10**, e0127182 (2015).
- 788 53. Tanaka, M. *et al.* Mitochondrial genome variation in eastern Asia and the peopling of
789 Japan. *Genome Res.* **14**, 1832–1850 (2004).
- 790 54. Ning, C. *et al.* Ancient Mitochondrial Genomes Reveal Extensive Genetic Influence of
791 the Steppe Pastoralists in Western Xinjiang. *Front. Genet.* **12**, 740167 (2021).
- 792 55. Matyushenko, V. I. & Sinitsina, G. V. Могильник у д. Ростовка вблизи Омска [Burial

- 793 Ground near the Village of Rostovka near Omsk].
794 <https://elibrary.ru/item.asp?id=24232508> (1988).
- 795 56. Fu, Q. *et al.* The genetic history of Ice Age Europe. *Nature* **534**, 200–205 (2016).
- 796 57. Raghavan, M. *et al.* Upper Palaeolithic Siberian genome reveals dual ancestry of Native
797 Americans. *Nature* **505**, 87–91 (2014).
- 798 58. Asko, P. LOCATION OF THE URALIC PROTO-LANGUAGE IN THE KAMA RIVER
799 VALLEY AND THE URALIC SPEAKERS' EXPANSION EAST AND WEST WITH THE
800 'SEJMA-TURBINO TRANSCULTURAL PHENOMENON' 2200-1900 BC. *Археология*
801 *евразийских степей* 258–277 (2022).
- 802 59. Grünthal, R. *et al.* Drastic demographic events triggered the Uralic spread. *Diachronica*
803 **39**, 490–524 (2022).
- 804 60. Kovtun, I. V. *Предыстория индоарийской мифологии [Prehistory of Indo-Aryan*
805 *mythology]*. (Азия-принт, 2013).
- 806 61. Saarikivi, J. The divergence of Proto-Uralic and its offspring. *The Oxford Guide to the*
807 *Uralic Languages* 28–58 Preprint at
808 <https://doi.org/10.1093/oso/9780198767664.003.0002> (2022).
- 809 62. A Fellows Yates, J. *et al.* A-Z of ancient DNA protocols for shotgun Illumina Next
810 Generation Sequencing v2. (2021) doi:10.17504/protocols.io.bvt9n6r6.
- 811 63. Fellows Yates, J. A. *et al.* Reproducible, portable, and efficient ancient genome
812 reconstruction with nf-core/eager. *PeerJ* **9**, e10947 (2021).
- 813 64. Jónsson, H., Ginolhac, A., Schubert, M., Johnson, P. L. F. & Orlando, L.
814 mapDamage2.0: fast approximate Bayesian estimates of ancient DNA damage
815 parameters. *Bioinformatics* **29**, 1682–1684 (2013).
- 816 65. Fu, Q. *et al.* A revised timescale for human evolution based on ancient mitochondrial
817 genomes. *Curr. Biol.* **23**, 553–559 (2013).
- 818 66. Renaud, G., Slon, V., Duggan, A. T. & Kelso, J. Schmutzi: estimation of contamination
819 and endogenous mitochondrial consensus calling for ancient DNA. *Genome Biol.* **16**,
820 224 (2015).
- 821 67. Korneliussen, T. S., Albrechtsen, A. & Nielsen, R. ANGSD: Analysis of Next Generation
822 Sequencing Data. *BMC Bioinformatics* **15**, 356 (2014).
- 823 68. Mallick, S. *et al.* The Allen Ancient DNA Resource (AADR): A curated compendium of
824 ancient human genomes. *bioRxiv* 2023.04.06.535797 (2023)
825 doi:10.1101/2023.04.06.535797.
- 826 69. Petr, M., Vernet, B. & Kelso, J. admixr—R package for reproducible analyses using
827 ADMIXTOOLS. *Bioinformatics* **35**, 3194–3195 (2019).
- 828 70. R Core Team, A., Team, R. C. & Others. R: A language and environment for statistical
829 computing. R Foundation for Statistical Computing, Vienna, Austria. 2012. Preprint at

- 830 (2022).
- 831 71. Wickham, H. *ggplot2: Elegant Graphics for Data Analysis*. (Springer International
832 Publishing, 2016).
- 833 72. Weissensteiner, H. *et al.* HaploGrep 2: mitochondrial haplogroup classification in the era
834 of high-throughput sequencing. *Nucleic Acids Res.* **44**, W58-63 (2016).
- 835 73. Peltzer, A. *et al.* EAGER: efficient ancient genome reconstruction. *Genome Biol.* **17**, 60
836 (2016).
- 837 74. Kolde, R. *pheatmap: Pretty heatmaps*. (Github, 2012).
- 838 75. Lazaridis, I. *et al.* Ancient human genomes suggest three ancestral populations for
839 present-day Europeans. *Nature* **513**, 409–413 (2014).
- 840 76. Damgaard, P. de B. *et al.* 137 ancient human genomes from across the Eurasian
841 steppes. *Nature* **557**, 369–374 (2018).
- 842 77. Fu, Q. *et al.* Genome sequence of a 45,000-year-old modern human from western
843 Siberia. *Nature* **514**, 445–449 (2014).
- 844